Progress In Electromagnetics Research C, Vol. 118, 61–70, 2022

Analysis of UUV Whip Antenna Radiated Power and Optimal Working Frequency in Seawater Environment

Menglei Xiu, Lihua Li*, Shimin Feng, Wenda Hou, and Longfei Wang

Abstract—In order to analyze the working status of the underwater unmanned vehicle not fully surfaced, the optimal working frequency when the whip antenna radiates the maximum power is given. The input impedance of the antenna on the water is theoretically calculated. It is regarded as the load of the underwater part of the antenna, and the total input impedance of the whip antenna is obtained. The relationship between the antenna radiated power to the external field and the input power is analyzed, and the optimal operating frequency corresponding to the maximum radiated power is determined. Using simulation experiments and actual measurements, the radiated power of the 1 m whip antenna when being immersed in seawater at 0.25 m, 0.5 m, 0.75 m is obtained, and the corresponding optimal working frequency is calculated, which are in good agreement with the theoretical deduction results. The results show that as the depth of the antenna immersed in seawater increases, the power radiated from the antenna to the external field decreases, and the optimal working frequency increases accordingly.

1. INTRODUCTION

Underwater Unmanned Vehicle (UUV) often completes various detection tasks underwater [1]. When the ocean exploration is completed, the data need to be transmitted to the receiving point [2]. In order to ensure a good communication effect, the underwater unmanned vehicle needs to empty the ballast tanks, float the hull, and transmit data through the whip antenna mounted on the top [3]. Considering the concealment and timeliness of the communication process, in many cases, the whip antenna is not exposed to the water surface as a whole, but a part of the upper end of the antenna is surfaced, and a higher frequency (such as VHF) electromagnetic wave is selected for work [4]. The working state of the underwater unmanned vehicle is shown in Figure 1. Due to frequent changes in the maritime environment, sometimes the transmitter and receiver cannot establish mutual communication. In order to improve the receiving field strength of the signal, it is necessary to make the whip antenna carried by the underwater unmanned vehicle radiate the maximum power when it floats to a certain height, so as to improve the signal-to-noise ratio of the received signal and reduce the received bit error rate [5].

It can be seen that the total length of the whip antenna is l; the length of the exposed part is l_1; and the antenna length is l_2 under seawater. In order to calculate the input impedance of the whip antenna when it rises above the surface of the water and determine the radiation power radiated to the external field, the impedance of the antenna on the sea surface needs to be considered. Combining the phase wavelengths of the voltage and current waves propagating on the transmission line in the seawater medium, find the equivalent circuits corresponding to the two parts [6–9]. In this way, the input impedance of the feeding point is obtained; the maximum radiated power is calculated; the corresponding optimal working frequency is found; and the accuracy of the calculation results is further proved through simulation software and physical experiments [10].

Received 23 December 2021, Accepted 20 January 2022, Scheduled 28 January 2022
* Corresponding author: Lihua Li (787220209@qq.com).
The authors are with the Department of Communication Engineering, Naval University of Engineering, Wuhan, Hubei 430000, China.

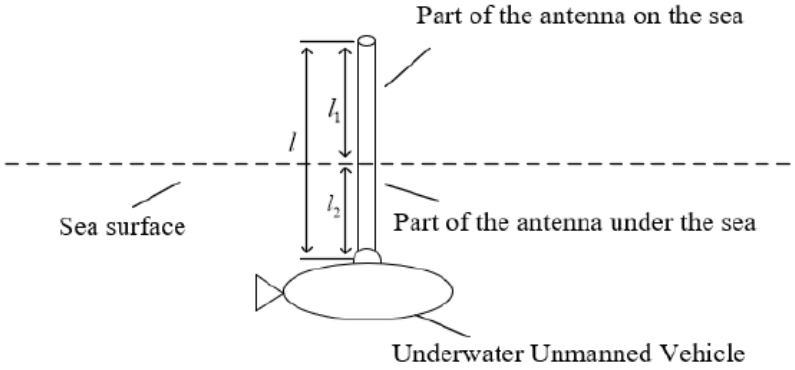

Figure 1. Diagram of the communication state of the underwater unmanned vehicle surfaced.

2. ANTENNA IMPEDANCE AND RADIATED POWER

2.1. Impedance of the Antenna on the Water

When the impedance of the antenna is calculated, the current distribution on the antenna is not an ideal sinusoidal distribution [11]. During the propagation of the current wave, the antenna part continuously radiates energy outwards, resulting in radiation loss [12]. In order to accurately calculate its impedance, the transmission line theory can be used to treat the antenna as a lossy transmission line with an average characteristic impedance [13]. In the working process of the whip antenna, it will form a symmetrical array with its mirror image of twice the antenna length [14]. The established antenna model of the water part is shown in Figure 2.

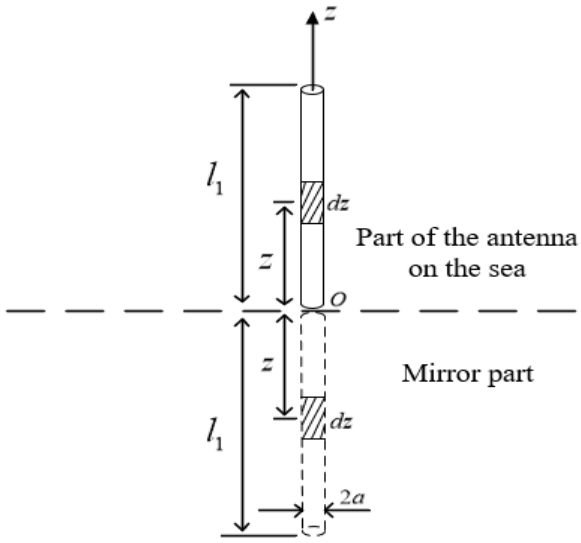

Figure 2. Antenna model of the surface part and mirror part.

For traditional uniform dual transmission lines, the characteristic impedance is [14]

$$Z_0 = 120\sqrt{\frac{\mu_r}{\varepsilon_r}}\ln\left(\frac{D}{a}\right) \tag{1}$$

Among them, μ_r is the relative permeability of the medium (take 1 for air medium), ε_r the relative permittivity (take 1 for air medium), D the distance between uniform double transmission lines, and a

the radius of the wire. At this time, the characteristic impedance corresponding to an antenna element dz of the whip antenna in the air should be $60\ln\left(\frac{2z}{a}\right)$ (1/2 of the characteristic impedance of a uniform double transmission line) [15], and the characteristic impedance value corresponding to each position is different. Integrating over the entire antenna length l_1, the average characteristic impedance of the antenna on the sea surface can be obtained as [16–18]

$$Z_{01} = \frac{1}{l_1}\int_0^{l_1} 60\ln\left(\frac{2z}{a}\right)dz = 60\left(\ln\frac{2l_1}{a} - 1\right) \tag{2}$$

The radiated power of the antenna at work can be regarded as the integral of the loss power of the loss resistance R_1 per unit length [19]. The power loss $\int_0^{l_1}|I(z)|^2 R_{01}dz$ should be equal to the radiated power $\frac{1}{2}|I_m|^2 R_{r1}$, which can be calculated

$$R_1 = \frac{2R_{r1}}{l_1\left(1 - \dfrac{\sin(2\beta_1 l_1)}{2\beta_1 l_1}\right)} \tag{3}$$

$I(z)$ represents the current value at any point of the antenna, I_m the current peak value, $R_{r1} = 12.35\left(\frac{4\pi}{\lambda}l_1\right)^{2.4}$ the radiation resistance [20], β_1 the phase shift constant of the lossy transmission line, and its value is $\frac{2\pi}{\lambda}\sqrt{\frac{1}{2}\left[1+\sqrt{1+\left(\frac{R_1\lambda}{2\pi Z_{01}}\right)^2}\right]}$.

The antenna on the sea surface can be equivalent to the terminal open-circuit condition of a uniform double transmission line [20], and its equivalent circuit is shown in Figure 3.

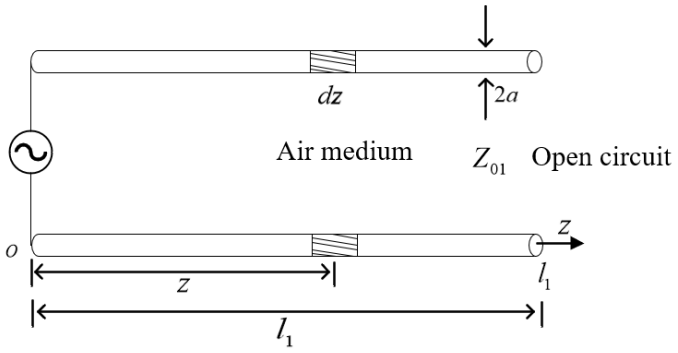

Figure 3. Open-ended circuit diagram of the equivalent uniform double transmission line of the antenna on the sea.

It can be obtained that the input impedance from any point of the antenna on the water is [21]

$$Z_{in}(z) = \frac{Z_{01}}{th[(\alpha_1 + j\beta_1)(l_1 - z)]} \tag{4}$$

where $\alpha_1 = \frac{R_1}{2Z_{01}}$ represents the antenna attenuation constant caused by the distributed resistance per unit length. The input impedance of the water part can be calculated as [22]

$$Z_{in}(0) = \frac{Z_{01}}{th[(\alpha_1 + j\beta_1)l_1]} \tag{5}$$

2.2. Impedance of Underwater Antenna

Under the premise of obtaining the antenna impedance on the water, it is necessary to calculate the antenna impedance of the underwater part to obtain the overall antenna impedance when the antenna is partially immersed in sea water. For underwater antennas, due to the good conductivity of seawater (the

dielectric constant of seawater is 80 and the magnetic permeability is 1), the characteristic impedance of the antenna will also change [23]. Similarly, the part below the seawater is equivalent to the double transmission lines in the seawater medium [24]. With reference to Equations (1)–(4), its characteristic impedance Z_{02} can be expressed as

$$Z_{02} = 6.7\left(\ln\left(\frac{2l_2}{a}\right) - 1\right) \tag{6}$$

The loss resistance per unit length is

$$R_2 = \frac{2R_{r2}}{l_2\left(1 - \dfrac{\sin(2\beta_2 l_2)}{2\beta_2 l_2}\right)} \tag{7}$$

The phase shift constant is

$$\beta_2 = \frac{2\pi}{\lambda/\sqrt{\varepsilon_s}}\sqrt{\frac{1}{2}\left[1 + \sqrt{1 + \left(\frac{R_2\lambda/\sqrt{\varepsilon_s}}{2\pi Z_{02}}\right)^2}\right]} \tag{8}$$

The attenuation constant is

$$\alpha_2 = \frac{R_2}{2Z_{02}} \tag{9}$$

The radiation resistance is

$$R_{r2} = 12.35\left(\frac{4\pi}{\lambda/\sqrt{\varepsilon_s}}l_2\right)^{2.4} \tag{10}$$

At this time, the entire whip antenna can be regarded as a double transmission line connected to a load impedance $Z_{in}(0)$ in the sea water medium [25], so that the antenna is in a traveling standing wave working state. The equivalent circuit is shown in Figure 4.

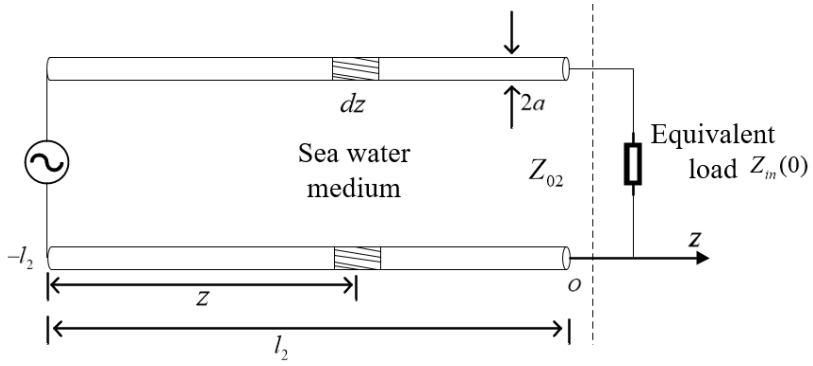

Figure 4. The terminal load circuit diagram of the equivalent uniform dual transmission line of the underwater antenna.

Viewed from the whip antenna feed to the end of the antenna, the total input impedance is

$$Z_{in}(-l_2) = \frac{Z_{in}(0) + Z_{02}th[(\alpha_2 + j\beta_2)l_2]}{Z_{02} + Z_{in}(0)th[(\alpha_2 + j\beta_2)l_2]} \tag{11}$$

2.3. Antenna Radiated Power

Considering that the input power of the whip antenna is determined, it is difficult for the radiated energy of the underwater antenna to be transmitted above the sea [26]. If the antenna on the sea is required to radiate the maximum power, the corresponding optimal working frequency should be considered from two aspects [27]: 1. The working frequency corresponding to the maximum power that

can reach the underwater antenna [28]; 2. After the antenna on the water receives the power transmitted by the underwater antenna, the working frequency corresponding to the maximum radiated power [29]. But often these two working frequencies are not equal, which means that the whole process of energy transfer from the bottom to the top of the whip antenna and radiated by the water antenna needs to be considered comprehensively, that is, the optimization problem of the optimal working frequency of the antenna [30]. At this time, if the voltage of the antenna feeding point is known, the power radiated by the antenna on the water can be quantified by the calculated antenna impedance.

Regarding the problem of receiving power at the surface, letting the input voltage of the underwater whip antenna feed point be $U(-l_2)$, the underwater feed point current can be $\frac{U(-l_2)}{Z_{in}(-l_2)}$, and the voltage and current values at point O are

$$U(0) = \frac{U(-l_2)+I(-l_2)Z_{02}}{2}e^{-(\alpha+j\beta)l_2} + \frac{U(-l_2)-I(-l_2)Z_{02}}{2}e^{(\alpha+j\beta)l_2} \tag{12}$$

$$I(0) = \frac{U(-l_2)+I(-l_2)Z_{02}}{2Z_{02}}e^{-(\alpha+j\beta)l_2} - \frac{U(-l_2)-I(-l_2)Z_{02}}{2Z_{02}}e^{(\alpha+j\beta)l_2} \tag{13}$$

The complex power of the point can be obtained from the voltage and current values of point O. The total input power is $P_{in}(-l_2) = \left|\frac{1}{2}U(-l_2)I^*(-l_2)\right|$, and the power that can reach the antenna on the water surface is

$$P_{in}(0) = \frac{1}{2}U(0)I^*(0) \tag{14}$$

The value of $P_{in}(0)$ does not represent the power that the antenna can radiate. The real part is the radiated power of the antenna, and the imaginary part represents a part of the power lost when the antenna on the water transmits energy. The radiated power of the antenna is $P_{\text{radiation}} = \text{Re}[P_{in}(0)]$, and the corresponding optimal working frequency is

$$P(\lambda_{\text{best}}) = \max[P_{\text{radiation}}(\lambda)] \tag{15}$$

3. SIMULATION

With the help of FEKO electromagnetic simulation software, the whip antenna model of the underwater unmanned vehicle is established. In order to prevent the exposed antenna from contacting sea water to

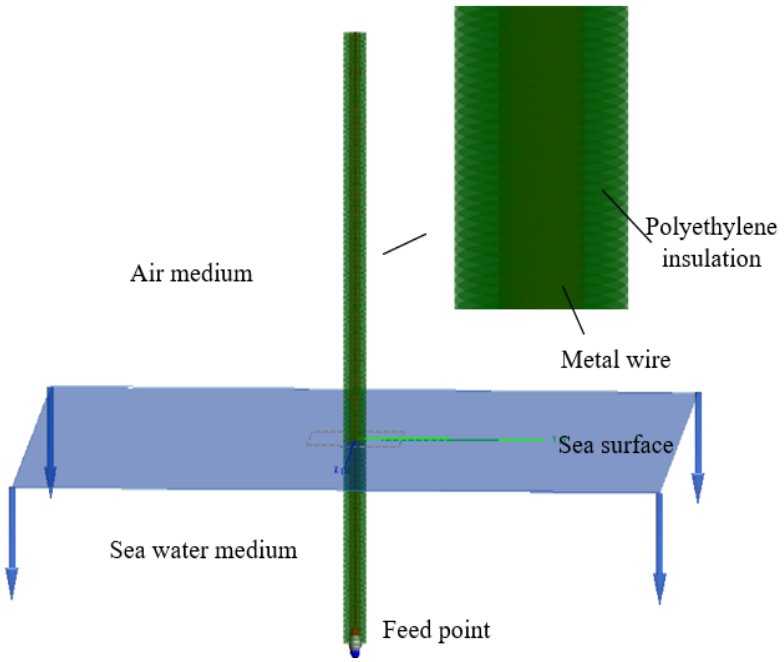

Figure 5. Simulation model of whip antenna.

affect the impedance characteristics, a 0.05 mm polyethylene insulating layer is filled on the outside of the whole antenna. The simulation model is shown in Figure 5.

With reference to the resonant frequency of a 1 m ideal whip antenna as 75 MHz, since the wavelength will become smaller in the seawater medium, the frequency will become larger accordingly. So the frequency of the simulation experiment is initially set in the 75–150 MHz frequency band, so as to observe the radiation power radiated to the external field and compare it with the calculated value to summarize the law. Without considering the front-end transmission line matching of the whip antenna, set the power input to the antenna to 10 W. It should be noted that it is meaningless to observe the reflection coefficient of the antenna, because it represents the matching degree of the entire whip antenna. The minimum reflection coefficient indicates that the antenna is in resonance, but the absorption capacity of the underwater antenna's radiated power is ignored. The simulation result is shown in Figure 6.

It can be seen from the figure that the radiated power decreases with the depth of the antenna immersed in the sea water, because the sea water absorbs the radiated energy of the underwater antenna.

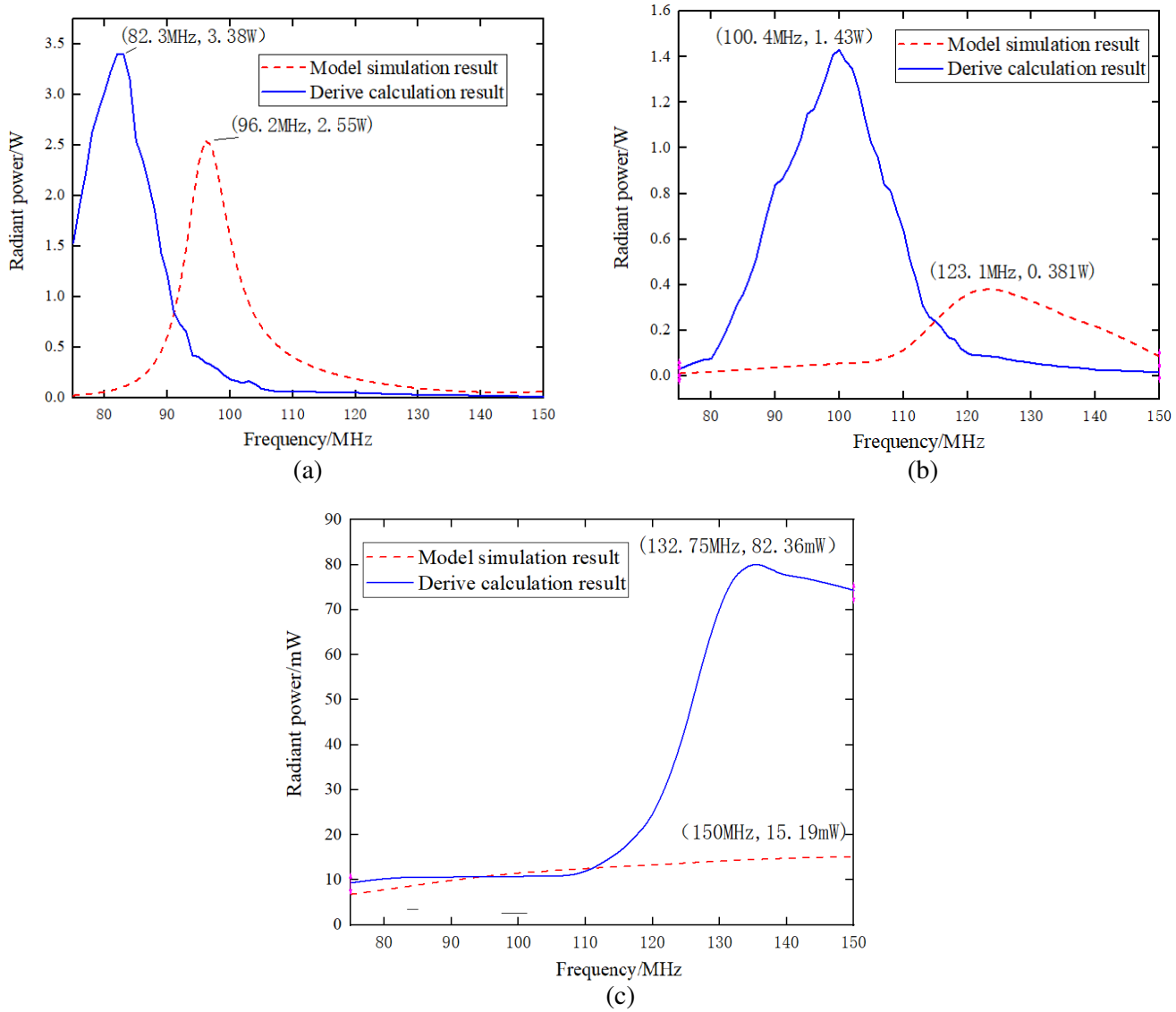

Figure 6. Comparison of simulation and theoretical calculation results. (a) Immersion depth 0.25 m; (b) Immersion depth 0.50 m; (c) Immersion depth 0.75 m.

As the immersion depth increases, the optimal working frequency increases correspondingly, because the sea water changes the impedance characteristics of the antenna, causing the antenna to resonate at a higher frequency. However, the optimal working frequency of the simulation is larger than the calculated value, which may be because the attenuation constant of the antenna uses a rough estimate, and the influence of the metal material on the current attenuation is weakened in the calculation. Therefore, the simulated value of the power radiated to the external field is slightly smaller than the calculated value.

4. PHYSICAL MEASUREMENT EXPERIMENT

In order to more accurately verify the correctness of the theoretical derivation and summarize the working rules of the underwater unmanned vehicle equipped with whip antenna when it rises to the surface, a physical model of the antenna is made, and a communication system is established. The transmitting device is shown in Figure 7.

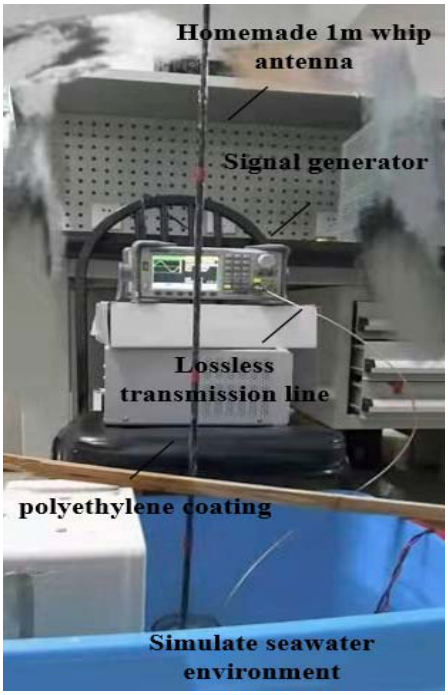

Figure 7. Self-made transmitting antenna device diagram.

In order to monitor the influence of the antenna immersion depth in seawater on the radiation efficiency, the antenna was immersed in 0.25 m, 0.5 m, and 0.75 m, respectively. Since the radiation power of the antenna is difficult to obtain a specific value through measurement, a loop antenna device is used to receive the signal at a distance of 500 m from the launch point. In order to avoid the influence of seawater contacting the antenna, a polyethylene coating is applied to the whip antenna. According to the basic characteristics of the whip antenna, theoretically at 75–150 MHz, the pattern of the 1 m whip antenna hardly changes, so the radiated power increases, and the received signal will increase accordingly. This shows that the received field strength value can be used indirectly to prove the consistency of the radiated power change. The power input to the antenna is 10 W. Considering that a certain amount of power will be reflected back from the actual transmitting antenna, it is necessary to use a network analyzer to calculate its reflection coefficient to ensure that the power input to the bottom of the antenna is 10 W. The measured receiving field strength at 500 m is shown in Table 1.

It can be seen that as the depth of the antenna immersed in the sea water continues to increase, the

Table 1. Receiving field strength at 500 m at different immersion depths.

Frequency (MHz)	Immersion depth: 0.25 m (mV/m)	Immersion depth: 0.50 m (mV/m)	Immersion depth: 0.75 m (mV/m)
75	19.83	4.43	0.642
8	24.47	5.24	0.647
85	**36.63**	5.31	0.652
9	36.04	5.36	0.668
95	35.17	6.34	0.670
100	33.13	6.51	0.672
105	26.87	**7.89**	0.674
110	22.19	7.25	0.678
115	18.77	6.46	0.682
120	16.37	6.31	0.684
125	14.37	5.79	0.706
130	12.35	5.67	**0.718**
135	11.30	4.12	0.693
140	10.14	3.34	0.631
145	9.27	2.24	0.587
150	8.43	5.08	0.526

received field strength continues to decrease, which indicates that the power radiated by the antenna to the external field is correspondingly reduced. At the same time, the optimal operating frequency increases, which maintains good consistency with the results of calculation and simulation, but there are still deviations. The reason may be that the seawater environment is not large enough, which causes the impedance of the antenna under water to deviate from the ideal value. But the optimal working frequency still maintains the same and good trend of change with the ideal value. Since the radiated power of the antenna obtained from the experiment is easily affected by the environment and receiving equipment, the receiving field strength can reflect the consistency of the optimal working frequency of the physical antenna with the calculation and simulation results, but the specific radiated power cannot be quantified, which is also a work that needs to be improved in the later stage.

5. CONCLUSION

Through theoretical calculation, simulation verification, and experimental measurement of the working state of a whip antenna mounted on an underwater unmanned vehicle, the optimal working frequency of the antenna at different depths immersed in seawater is obtained. The results show that as the depth of the antenna immersed in seawater increases, the power that the antenna can radiate to the external field decreases, and the optimal working frequency increases accordingly. It shows that the seawater medium not only absorbs the radiated power of the underwater antenna, but also changes the impedance value of the antenna. Therefore, it is necessary to consider the power component of the antenna input power reaching the antenna on the water surface and the maximum power it can radiate, so as to determine the corresponding optimal working frequency, which provides an application basis and theoretical basis for the operation of the offshore surface antenna.

ACKNOWLEDGMENT

This work was supported by the National Natural Science Foundation of China (41774021; 41874091; 42074074) and the Innovation Fund of the Naval University of Engineering (HGCXJJ2019015).

REFERENCES

1. Zhang, X., M. Han, Y. Yu, T. Huang, and Q. Chen, "The development status and key technologies of cooperative combat between submarine and UUV," *Journal of Underwater Unmanned Systems*, Vol. 29, No. 5, 497–508, 2021.
2. Ma, Y. and L. Wang, "Research on multi-frequency and multi-notch antenna loaded with metamaterials," Xi'an University of Technology, 2021.
3. Ma, L., J. Zhang, X. Sun, and T. Luan, "Research on UUV underwater communication networking technology based on ad hoc mode," *Digital Technology and Application*, Vol. 39, No. 6, 24–26+30, 2021.
4. Wang, H., "Analysis of the research status of submersible UUV," *Digital Ocean and Underwater Attack and Defense*, Vol. 4, No. 5, 351–356, 2021.
5. Zhao, Y., H. Peng, and Q. Li, "Analysis of antenna impedance and radiation efficiency partially submerged in seawater," *Chinese Journal of Radio Science*, Vol. 36, No. 4, 518–523, 2021.
6. Qu, S., C. Wu, L. Ye, and Y. Yang, "Distance measurement and timing system between UUVs based on underwater acoustic link," *Communication Technology*, Vol. 54, No. 6, 1356–1362, 2021.
7. Qi, L., B. Liu, and G. Kan, "Study on the validity of several rough scattering theories on sea surface intermediate frequency backward scattering," *Journal of Ocean University of China (Natural Science Edition)*, Vol. 51, No. 1, 94–102, 2021.
8. Li, Z., "Selection of short-wave communication antennas for marine buoys," *China Water Transport*, Vol. 11, No. 7, 2011.
9. Wang, H., C. Liu, H. Wu, and X. Xie, "A novel broadband double whip antenna for very high frequency," *Progress In Electromagnetics Research C*, Vol. 99, 209–219, 2020.
10. Li, J., Y. Li, J. Dong, and X. Wang, "Polarization characteristics analysis of crossed dipoles," *Chinese Journal of Radio Science*, Vol. 27, No. 2, 396–401+424, 2012.
11. Wang, S., L. Li, Y. Zhang, and Y. Wang, "Application analysis of similarity principle in the design of the underwater receiving antenna," *Progress In Electromagnetics Research M*, Vol. 95, 189–197, 2020.
12. Bai, Q., "Dynamic analysis and structural optimization of marine buoys and antenna masts," Ocean University of China, 2008.
13. Li, Z., "A brief talk on the application of sea-land microwave antenna multiplexing system in offshore oil platforms," *China New Communications*, Vol. 23, No. 8, 101–104, 2021.
14. Hu, Y., K. Zhang, and C. Xing, "Ship dim target detection based on sea antenna," *Journal of Northwestern Polytechnical University*, Vol. 37, No. 1, 35–40, 2019.
15. Sun, D., H. Rong, and J. Zhang, "Satellite buoy antenna technology and its application in submarine communication," *Equipment Environmental Engineering*, Vol. 6, No. 5, 54–56+67, 2009.
16. Liu, B. and K. Luo, "Design of wireless monitoring buoy antenna in underwater acoustic positioning system," *Ship Electronics Engineering*, Vol. 38, No. 11, 183–185, 2011.
17. Li, R., "Research on wireless communication network planning technology in naval battlefield," *Ship Electronics Engineering*, Vol. 32, No. 8, 64–66, 2012.
18. Shi, Z., Y. Zhao, X. Qu, and L. Ma, "High-efficiency simulation calculation of electromagnetic field radiated by layered ocean electrical antennas," *Aerospace Electronic Warfare*, Vol. 27, No. 3, 13–23, 2021.
19. Nie, Z., *Antenna Engineering Manual*, University of Electronic Science and Technology Press, 2014.
20. Han, G., G. Chen, J. Lu, and Y. Lin, "Tetra net-based container logistics wireless communication platform — Realizing the logistics system "Sea and land connection, world and earth integration,"" *Journal of Shanghai Maritime University*, 14–20, 2016.
21. Ju, Y., S. Lei, and Y. Xue, "A design of ultra-wideband antenna based on hypermedia," *Journal of Dalian Jiaotong University*, Vol. 42, No. 5, 100–105, 2021.
22. An, W., W. Zhao, and Y. Luo, "Design of low sidelobe cubic mode compression dipole antenna," *Journal of Hunan University (Natural Science Edition)*, 209–211, 2021.

23. Wang, S., L. Li, L. Wang, T. Fu, and S. Feng, "Electrical characteristics analysis of a new dual-radiator antenna in Ku band," *Chinese Journal of Radio Science*, 1–8, 2021.
24. Wang, J., "Research on a new type of ultrashort wave omnidirectional conformal antenna," University of Science and Technology of China, 2021.
25. Wang, H., C. Liu, X. Xie, and H. Wu, "A novel HF broadband frequency-reconfigurable whip antenna with radiation blades loading," *IEEE Access*, Vol. 7, 168944–168955, 2019.
26. Ren, X., X. Wei, W. Yang, H. Xu, and T. Jiang, "Analysis of the propagation characteristics of deep sea surface communication channel," *Communication Technology*, Vol. 54, No. 6, 1314–1319, 2021.
27. Wang, H., C. Liu, X. Xie, and H. Wu, "Gain-improved VHF broadband whip antenna loaded with radiation blades," *IET Microwaves Antennas & Propagation*, Vol. 14, No. 12, 1446–1454, 2020.
28. Liu, J., "Impedance characteristic analysis of dipole antenna," *Chinese Journal of Radio Science*, Vol. 28, No. 6, 1205–1211, 2013.
29. Wen, Y., "Antenna and radio wave propagation theory," *Safety & EMC*, 2005.
30. Ruan, Y., "Calculation of the input impedances of cylindrical doublet antennae by the application of the static electricity and transmission line theories: An amendment to the equivalent transmission line method," *Journal on Communications*, 1981.